Numerical studies of critical percolation in three dimensions

1992 J. Phys. A: Math. Gen. 25 5867

(http://iopscience.iop.org/0305-4470/25/22/015)

J. Phys. A: Math. Gen. 25 (1992) 5867–5888. Printed in the UK

Numerical studies of critical percolation in three dimensions

P Grassberger

Physics Department, University of Wuppertal, D-5600 Wuppertal 1, Federal Republic of Germany

Received 22 May 1992

Abstract. We present results of high-statistics simulations of the spreading of 3D percolation close to the critical point. Our main results are (i) a more precise estimate of the spreading (resp. 'chemical distance') dimension; (ii) a novel heuristic scaling theory for percolation near surfaces; and (iii) more precise values for critical surface and edge exponents. In adition, we verify the very precise results of Ziff and Stell for the percolation thresholds, and we study in detail corrections to scaling. The latter is made possible by simulating bond *and* site percolation, in a number of different geometries. In addition, in most cases we could measure more than one observable during each simulation, which provided us with quite severe internal consistency constraints. In some cases, we found quite important deviations from scaling which are not easily described by a single power or logarithmic correction term.

1. Introduction

The percolation problem provides us with one of the simplest and most intuitive critical phenomena (for a review, see [1]). It is thus not surprising that its critical behaviour has been studied *in extenso*. Tools for this include the field theoretic renormalization group (mostly near six dimensions), series expansions, conformal invariance and exactly solvable models (in two dimensions) and simulations. In three dimensions, which will be the case studied exclusively in this paper, the most precise results have been obtained with Monte Carlo simulations. In particular, there even exist special purpose computers such as the machine 'percola' at Saclay [2] which were built and run exclusively in order to get more precise results on the critical behaviour.

The critical exponents most difficult to measure (and those measured in [2], in particular; see also [3–5]) are exponents related to conductivity and elastic properties of the critical networks. For the basic 'classical' critical exponents and the percolation thresholds, the most extensive simulations up to now have been made by Ziff and Stell [6]. They used several low-cost desktop computers 'for extended periods of time' to get $p_c = 0.2488125 \pm 0.0000010$ for bond percolation and $p_c = 0.311605 \pm 0.000010$ for site percolation, both on simple cubic lattices. Note that the algorithms used in [6] and in the present paper are neither vectorizable nor parallelizable, whence the optimal computing environment for them are desktop workstations.

The most serious problem with all numerical studies of critical phenomena are possible corrections to scaling. The underestimation of deviations from the asymptotic

0305-4470/92/225867+22$07.50

scaling laws is mostly responsible for the large number of wrong estimates of critical exponents existing in the literature. The work on percolation (and some of my own previous work) is no exception in this respect.

The possible problems due to deviations from scaling are best illustrated by an example. This example indeed stimulated the present investigation, and the situation underlying it is the basic model studied in this paper.

Consider the spreading of an epidemic process (the 'bug in the orchard' of Broadbent and Hammersley [7]) at the critical point, i.e. in a medium where the epidemic can just barely survive. Assume that the epidemic can spread just to the next neighbour during one time step, and that each site can remain infective during one time step, too. After that, the site remains immune. This process is called 'general epidemic process' [8, 9], and a site infected at time t is called a 'growth site' at this time. The set of all growth sites at a given time t is exactly the set of sites connected to the 'seed' of the epidemic by minimal paths of length t. Here the seed is the set of sites infected at $t = 0$. The set of all sites which will be growth sites at any time forms the infinite percolation cluster.

In particular, consider a configuration where the seed consists of all sites on a straight line, and where the epidemic spreads essentially radially away from this line. At the critical point we expect that the average distance of the growth sites from the seed and the average number of growth sites per unit of length of the seed should both increase as powers of t,

$$R \sim t^z \qquad n_g \sim t^y. \tag{1}$$

Later we will discuss these scaling laws in more detail, and will relate the exponents z and y to more conventional critical indices. For the moment we just present results of simulations for R and n_g against t. In figure 1 n_g against t is shown on a log–log scale. Results for bond and site percolation are given, for a number of values of p very close to the respective p_c. While the results for bond percolation are perfectly consistent with no corrections to scaling (for $t > 10$), this is obviously not so for the site percolation results. If we had the latter alone (and if we had somewhat lower statistics—with our very high statistics the fit is not very good), we would get a straight-line fit for $p \approx 0.3117$–0.3118. If we would accept this fit, we would get a much higher value of y than before, and thus a very serious violation of universality. The latter tells us that the exponent y is the same in bond and site percolation, and thus the lines in figure 1 should become parallel asymptotically. We thus conclude that p_c for site percolation must be near 0.3116, in agreement with [6], and that the curvature seen in figure 1 is due to very large corrections to scaling. Notice that this conclusion is reached only since we had also the bond data available as a consistency check.

The values of R depend much less strongly on the precise value of p, and have much smaller statistical errors. We will plot $\log R$ against $\log t$ later (figure 3), but in figure 2 we show the effective slopes in such a plot, obtained by fitting straight lines over intervals $[t/4, t]$. If the corrections to equation (1) were dominated by analytic terms (which can be absorbed into a time offset t_0; $t' = t - t_0$) plus a single power,

$$R = A\, t'^z \left(1 + \frac{b}{t'^\Delta} + \ldots\right) \tag{2}$$

then we would get straight lines when plotting $\mathrm{d}\log R/\mathrm{d}\log t'$ against $1/t'^\Delta$. We found that the value of Δ which gave the best straight lines is ≈ 0.6, and

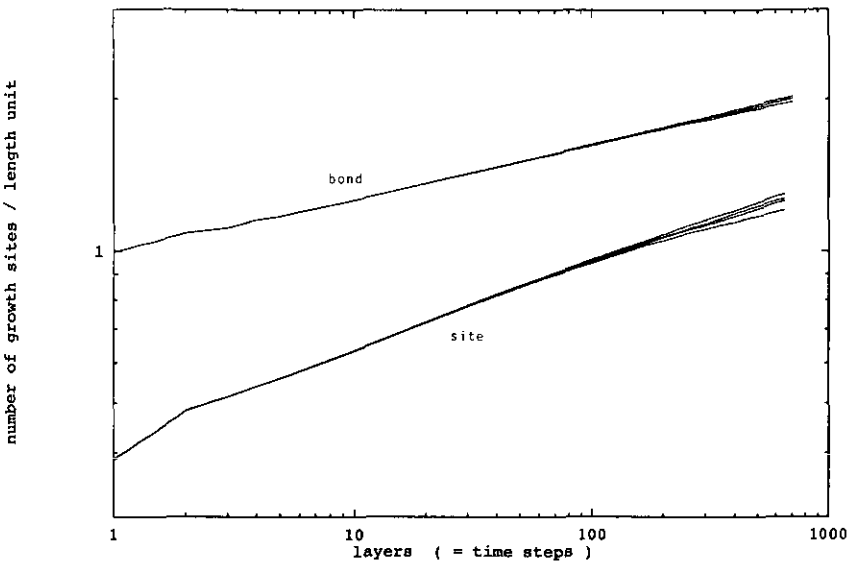

Figure 1. Average number of growth sites plotted against time for spreading from a line seed. The upper set of curves corresponds to bond percolation, with $p = 0.24880$, 0.24881 and 0.24882. The lower curves are for site percolation with $p = 0.31155$, 0.31160, 0.31162 and 0.31165. Statistical errors are less than the thickness of the lines.

thus plotted in figure 2 the slopes against $1/t'^{0.6}$. We see now that the most straightforward extrapolation would again give different critical exponents for site and bond percolation, but now the difference cannot be blamed on the precise values of p_c. Obviously there are important deviations from scaling not taken into account by equation (2). As suggested already by figure 2 and confirmed by a more serious analysis, they cannot be fitted with a single logarithmic correction term instead of a power law, as proposed for a similar problem in [10].

In view of these observations, it seems that the safest way to find all systematic deviations from scaling—and thus the correct critical exponents — is to study at the same time a large number of observables in many different circumstances. For this reason, we present in this paper results both for site and for bond percolation. In all simulations except the last ones (discussed in subsections 3(*b*) and 4(*c*)), we study spreading phenomena, with the observables measured as functions of the time t. We use a number of different seeds: line seeds as above, point seeds and seeds which consist of all sites in an entire plane. The observables we measure in all these cases are the numbers of growth sites and their distances from the seed. In cases where the spreading can stop since the seed had non-vanishing overlap with the incipient infinite cluster, we measure also the probability $P(t)$ that the spreading has not yet stopped (that the epidemic has not yet died out). Finally, we take not only seeds in the interior of very large lattices, but also seeds on surfaces. In this way we can also measure surface critical exponents.

As anticipated, the results of all these measurements are not compatible with pure scaling laws. They are also not compatible with the assumption that in all cases the deviation from scaling is described by a single power or logarithm. Nevertheless, we will find that taken together they give by far the most precise estimates of the

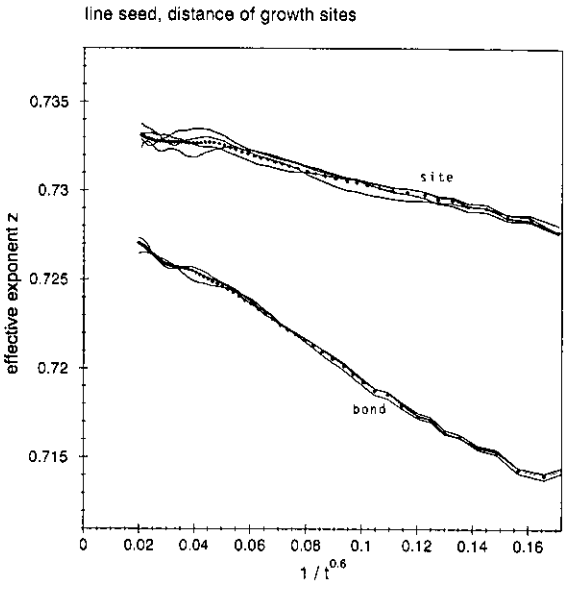

Figure 2. Effective exponents for the increase of the distance of the growth sites from a line seed. The values of p are the same as in figure 1, with the upper curves corresponding to site percolation, and the lower ones to bond percolation. The dots correspond to averages over p which coincide with the values of p_c given in [6]. The data were obtained by fitting straight lines to intervals with $t_{max}/t_{min} = 4$. The leading analytic correction is taken into account by using $t - t_0$ instead of t, and the data are plotted against $1/t^{0.6}$ since this gave the straightest lines. The statistical errors are as illustrated by the fluctuations of the curves.

spreading exponent and of surface exponents up to the present. They also give very precise estimates for p_c, in good agreement with those of [6].

In the next section we shall formulate the relevant scaling laws. Part of the scaling ansatz for spreading in the vicinity of a surface seems to be new. In section 3 we describe the simulations. Their results are discussed in section 4, and in section 5 we draw our conclusions.

2. Scaling laws for spreading

The relevant scaling laws have been formulated for special seeds in [9, 11, 12], and our generalization will be straightforward. In the next subsection we assume that the seed is finite and is in the interior of an infinite lattice. Spreading from infinite seeds will be studied in subsection 2(b) and spreading in the vicinity of a surface will be considered in subsection 2(c).

2(a) *Bulk behaviour, finite seeds.* Let us denote the seed by $\mathcal{S}$. It is a finite subset of sites from the cubic lattice Z^3. The basic quantity for which scaling laws are formulated are as follows.

(i) the density of growth sites $\rho(\boldsymbol{x}, t, \epsilon|\mathcal{S})$ at time t and point $\boldsymbol{x}$, with $\epsilon = p - p_c$. We assume that spreading started at $t = 0$, and we define the distance r of $\boldsymbol{x}$ from the seed as $r = \min_{\boldsymbol{y}\in\mathcal{S}} ||\boldsymbol{x} - \boldsymbol{y}||$, where $||\cdot||$ denotes the Euclidean norm. From

$\rho(x,t,\epsilon|\mathcal{S})$ we can immediately obtain the average nunmber $N_g(t,\epsilon|\mathcal{S})$ and the average distance $r(t,\epsilon|\mathcal{S})$ of growth sites by integration.

(ii) the probability $P(t,\epsilon|\mathcal{S})$ that the set of growth sites is non-empty at time t.

Using renormalization group ideas, we expect that the asymptotic behaviour is the same for any *finite* seed, and we have the ansatzes

$$\rho(x,t,\epsilon|\mathcal{S}) \approx \frac{\epsilon^{2\beta}}{t} F(r/t^z, \epsilon t^{1/\nu_t}) \tag{3}$$

and

$$P(t,\epsilon|\mathcal{S}) \approx \epsilon^{\beta} G(\epsilon t^{1/\nu_t}). \tag{4}$$

These ansatzes need some comments.

Firstly, the scaling variable r/t^z in equation (3) leads directly to the scaling law $R \approx t^z$ encountered already in the introduction, for any seed (we just have to assume that the scaling function $F(x,y)$ is smooth in x and integrable).

Secondly, the dependence on ϵ is more conventionally written by means of the scaling variable $t\epsilon^{\nu_t}$. Our ansatz has the advantage that $F(x,y)$ and $G(y)$ have simple analyticity properties in y near $y = 0$ [9], as will be discussed below. Using instead $t\epsilon^{\nu_t}$ as scaling variable would lead to a more complicated singularity of the scaling functions at the origin.

The prefactor ϵ^{β} in equation (4) is obtained by considering the limit $t \to \infty, \epsilon =$ constant > 0, and by assuming the scaling function $G(y)$ to be finite for $y \to \infty$. In this limit, $P(t,\epsilon|\mathcal{S})$ becomes equal to the probability $P(\epsilon,\mathcal{S})$ that the seed intersects with the infinite cluster. This probability should have the same scaling behaviour for all finite seeds, namely $\sim (p - p_c)^{\beta}$.

Finally, the prefactor $\epsilon^{2\beta}/t$ in equation (3) has a similar origin: one factor ϵ^{β} comes from the above probability that the seed intersects with the infinite cluster, while the remaining factor ϵ^{β}/t comes from the probability that the site at x is in the infinite cluster too. The infinite cluster is just the set of all points which act as growth sites at any time. Thus the probability for a distant x to be in the infinite cluster is given by

$$\lim_{r\to\infty} \frac{1}{P(\epsilon,\mathcal{S})} \int_0^{\infty} \mathrm{d}t\, \rho(x,t,\epsilon|\mathcal{S}) \equiv \lim_{r\to\infty} P(\epsilon,x) \sim \epsilon^{\beta}. \tag{5}$$

To obtain the behaviour exactly at the critical point (this is what we are mostly interested in), we write

$$F(x,y) = y^{2\beta} f(x,y) \qquad G(y) = y^{\beta} g(y) \tag{6}$$

so that equations (3) and (4) become

$$\rho(x,t,\epsilon|\mathcal{S}) \approx t^{-2\beta/\nu_t - 1} f(r/t^z, \epsilon t^{1/\nu_t}) \tag{7}$$

and

$$P(t,\epsilon|\mathcal{S}) \approx t^{-2\beta/\nu_t} g(\epsilon t^{1/\nu_t}). \tag{8}$$

We can now assume that $f(x, y)$ and $g(y)$ are finite (and analytic) at $y = 0$, and obtain

$$\rho(x, t, 0|\mathcal{S}) \sim t^{-2\beta/\nu_t - 1} f(r/t^z, 0) \tag{9}$$

and

$$P(t, 0|\mathcal{S}) \sim t^{-\delta} \tag{10}$$

with

$$\delta = \beta/\nu_t. \tag{11}$$

Integrating over x at fixed t (in d dimensions of space) we obtain from equation (9)

$$N_g(t, 0|\mathcal{S}) = \int \mathrm{d}^d x\ \rho(x, t, 0|\mathcal{S}) \sim t^{y_{\text{point}}} \tag{12}$$

with

$$y_{\text{point}} = dz - \frac{2\beta}{\nu_t} - 1. \tag{13}$$

This can also be written as $y_{\text{point}} = \hat{d} - \beta/\nu_t - 1$, where

$$\hat{d} = dz - \beta/\nu_t \tag{14}$$

is the 'spreading dimension'. When conditioning on seeds which overlap with the infinite cluster, then the total number of sites 'wetted' at times $\leqslant t$ scales as $t^{\hat{d}}$.

Finally, it is easily seen that

$$z = \nu/\nu_t \tag{15}$$

where ν describes the correlations between points in the infinite cluster [1]. For this we have just to consider the integral of $\rho(x, t, \epsilon|\mathcal{S})$ over all $t > 0$ at fixed x, and find that it is a function of the scaling variable $\epsilon r^{1/\nu}$, up to a pure power. The fractal dimension D_f of the infinite incipient cluster is $D_f = \hat{d}/z = d - \beta/\nu$.

2(*b*) *Bulk behaviour, infinite seeds.* Apart from having different scaling functions, the main difference when going over to infinite seeds is that the seed has a larger chance to intersect with the infinite cluster.

It is known that in three dimensions the critical infinite cluster has fractal dimension $D_f \approx 2.5$ [11]. Thus the intersection of a line with it will have $D_f \approx 0.5$, and the intersection with a plane has $D_f \approx 1.5$. Since both are positive, a typical line or plane will intersect the infinite cluster with probability 1, and we find that $P(t, \epsilon) = 1$ for line and plane seeds. The same is true in four dimensions where $D_f \approx 3.05$ [11]. Notice that this applies only to infinite seeds. On finite lattices one has strong cross-over effects. Finally, for dimensions greater than four the line will

not intersect the infinite cluster with probability 1, and the following arguments will have to be replaced by ones similar to those leading to equation (29) below.

For the density $\rho(x,t,\epsilon|\mathcal{S})$, this means that the prefactor $\epsilon^{2\beta}/t$ in equation (3) has to be replaced by ϵ^{β}/t. When considering the number of growth sites, we have to take into account that we must study the average number *per unit length* resp. unit surface, not the absolute number. We call this n_g. For a line seed, we thus obtain

$$n_g(t,0|\mathcal{S}=\text{line}) = \int \mathrm{d}^{d-1}x_\perp\ \rho(x_\perp,t,0|\mathcal{S}=\text{line}) \sim t^{y_{\text{line}}} \tag{16}$$

with [12]

$$y_{\text{line}} = (d-1)z - \frac{\beta}{\nu_t} - 1. \tag{17}$$

For a plane seed, we find similarly

$$n_g(t,0|\mathcal{S}=\text{plane}) = \int \mathrm{d}^{d-2}x_\perp\ \rho(x_\perp,t,0|\mathcal{S}=\text{plane}) \sim t^{y_{\text{plane}}} \tag{18}$$

with [9]

$$y_{\text{plane}} = (d-2)z - \frac{\beta}{\nu_t} - 1. \tag{19}$$

More generally, we could also consider fractal seeds. The resulting densities would in general depend non-trivially on the direction of x. Studying this would go beyond the scope of the present paper.

2(*c*) *Surfaces and edges.* If the spreading is away from a surface, the above ansatzes remain essentially unchanged, even if the seed happens to be located on the surface. The only modifications (again apart from different scaling functions) are that the spreading might become direction dependent, and that the exponent β is different on a surface. In the following we shall assume the surface to be straight.

It is well established that the probability that a surface site is contained in the infinite cluster in the supercritical case scales as [13–16]

$$P(\epsilon, x \in \text{surface}) \sim \epsilon^{\beta_s} \tag{20}$$

with a new exponent $\beta_s > \beta$. A surface site is less likely to be connected to the infinite cluster since all connecting paths which would have passed outside the surface are cut off.

Let us now consider the spreading from a point seed located on a surface. Equation (4) now has to be replaced by

$$P(t,\epsilon|\text{surface point}) \approx \epsilon^{\beta_s} G_s(\epsilon t^{1/\nu_t}). \tag{21}$$

where G_s is a new scaling function, but the critical exponent ν_t is not changed. At criticality, we have thus $P \sim t^{-\delta_s}$ with

$$\delta_s = \beta_s/\nu_t \tag{22}$$

in analogy to equations (11).

On an edge characterized by an angle θ, we expect that β is replaced by a function of θ. In particular, for a rectangular edge (which is the only case studied below) we shall call the critical exponent $\beta_{\rm edge}$, and expect that $\beta_{\rm edge} > \beta_{\rm s}$. In analogy to the above, the growth survival probability for a point seed on such an edge will decrease as $P \sim t^{-\delta_{\rm edge}}$ with $\delta_{\rm edge} = \beta_{\rm edge}/\nu_t$.

The density of growth sites in the vicinity of a plane surface will scale differently parallel to the surface and away from it. Let us denote by ϕ the angle between the growth direction and the surface. Then equation (3) is replaced by

$$\rho(x,t,\epsilon|\text{surface point}) \approx \begin{cases} \epsilon^{(\beta+\beta_s)/t} F_s(r/t^z, \epsilon t^{1/\nu_t}, \phi) & \text{for } \phi \neq 0 \\ \epsilon^{(2\beta_s)/t} F_{ss}(r/t^z, \epsilon t^{1/\nu_t}) & \text{for } \phi = 0. \end{cases} \tag{23}$$

Notice that we assume also that the exponent z is unchanged. The fact that the exponents ν and ν_t are unchanged in the vicinity of a surface were previously derived by field theoretic methods in [13] and [14], respectively. The simulations presented below give another independent and numerically very precise verification.

From these ansatzes it follows that the average distance of growth sites from the seed increases at the critical point as t^z, both for growth sites on the surface and in the bulk. This might seem surprising since the 'static' critical correlations between surface sites decrease faster with distance than in the bulk: $c(x) \sim r^{2-d+\eta_s}$ with $\eta_s = 2\beta_s/\nu - d - 2$. Also the fractal dimension of the set of wetted surface sites, $D_{f,s} = d - 1 - \beta_s/\nu$, is different from that in the bulk. But in spite of that, the clusters of all wetted sites are not very non-isotropic. The ratio $\langle R_\perp^2\rangle/\langle R_{||}^2\rangle$ is only ≈ 1.25, and the main anisotropy is concentrated in a rather thin region near the surface.

This faster decay of 'static' correlations arises from the fact that the number $N_g^{\rm surf}$ of growth sites on the surface decreases faster than that of growth sites in the bulk. From equation (23) we obtain

$$N_g(t,0|\text{surface point}) \sim t^{y_{\rm surf}} \qquad y_{\rm surf} = dz - \frac{\beta+\beta_s}{\nu_t} - 1 \tag{24}$$

and

$$N_g^{\rm surf}(t,0|\text{surface point}) \sim t^{y_{\rm surf,surf}} \qquad y_{\rm surf,surf} = (d-1)z - \frac{2\beta_s}{\nu_t} - 1. \tag{25}$$

For point sources on edges, one has analogously

$$y_{\rm edge} = dz - \frac{\beta+\beta_{\rm edge}}{\nu_t} - 1 \tag{26}$$

$$y_{\rm edge,surf} = (d-1)z - \frac{\beta_s+\beta_{\rm edge}}{\nu_t} - 1 \tag{27}$$

and similarly for $y_{\rm edge,edge}$.

Finally, the density of surface sites which are connected to any site a distance L away from the surface (and whence are wetted though a slab of finite thickness L) is found to decrease at criticality as [15, 16]

$$\rho \sim L^{-\beta_s/\nu}. \tag{28}$$

In addition to point seeds on surfaces, we had also studied in [12] line seeds on surfaces and on edges between perpendicular surfaces. In these cases the survival probability $P(t)$ would still be 1 on an infinite lattice, but its behaviour will be complicated on finite lattices. The growth site number, on the other hand, will scale with exponents which depend on the fractal dimension of wetted boundary (resp. edge) sites.

The fractal dimension D_{edge} of wetted edge sites is definitely less than zero for $d = 3$ [12] (i.e. the probability that an edge contains a site in the infinite cluster decreases as an inverse power of the lattice size). The scaling exponent can then be estimated as follows. Let us consider those sites on the edge which are connected to clusters reaching a distance ξ away from the edge. A site will belong to this set essentially if the spreading from it survives at least a time $t = \xi^{1/z}$. The density of such sites will thus decrease as $\xi^{-\beta_{\text{edge}}/\nu}$. On the other hand, each such site will give rise to a roughly isotropic cluster of growth sites with $\sim \xi^{D_t}/t = t^{\hat{d}-1}$ sites. These clusters will essentially not overlap if $\beta_{\text{edge}} > \nu$. In this case the total number of growth sites per unit length $n_g(t, 0 \,|\, \text{edge line})$ should scale with an exponent which is exactly that for a point seed on the edge,

$$y_{\text{edge line}} = \hat{d} - 1 - \beta_{\text{edge}}/\nu_t = dz - \frac{\beta + \beta_{\text{edge}}}{\nu_t} - 1 = y_{\text{edge}}. \tag{29}$$

Notice that this would also agree with equation (17) if $\beta_{\text{edge}} = \nu$, i.e. if the non-overlap condition would hold marginally. The non-overlap condition is just the condition that $D_{f,\text{edge}} < 0$.

In contrast to edge sites, the fractal dimension of the set of surface sites $D_{f,s}$ is very close to 1 (for $d = 3$) [12]. Thus its intersection with a line has dimension very close to zero. In this case it is not clear *a priori* whether $y_{\text{surf line}} = y_{\text{surf}}$ (if $D_{f,s} < 1$) or whether $y_{\text{surf line}} = y_{\text{line}}$ (if $D_{f,s} > 1$).

3. The simulations

(*a*) As we had already said in the introduction, all simulations (except those described in part (*b*) below) model the growth processes described in the last section. They use essentially the same routines as those in [11, 12], with just a few technical improvements which increase speed. In particular, the status of each site (wetted/not-wetted for bond percolation, tested/not tested for site p) is stored in 1 bit (using multispin-coding, i.e. storing 32 sites in one long integer word). The list of actual growth sites is stored in an array which is updated and replaced after each time step. The random decision whether a site (resp. bond) is broken or not is not made in advance but 'on the fly'. Thus it has to be made only for sites (bonds) which have at least one wetted neighbour. On large lattices this is a very important saving, making the routine much faster than the well-known Hoshen–Kopelman algorithm, for

example. This algorithm is often called the Leath algorithm, though the description given by Leath [17] is somewhat different and, when followed literally, would be much slower. As random number generator we used a Kirkpatrick–Stoll type generator [18] with $(p, q) = (250, 147)$. On a DECstation 2100, where most of the simulations were done, we got about 50000 wetted sites per second for bond percolation, and 30000 for site percolation. For a bond cluster obtained from a point seed and followed for up to 800 time steps, this gave on average about 0.365 s.

In order to avoid excessive swapping, the lattice sizes actually used by most clusters were typically restricted to about 10^6 sites (12 MB). The allocated lattices were defined to be about twice as large, to allow larger clusters occasionally and thus to avoid finite-size effects.

Let us now consider possible finite-size corrections (FSCs) in more detail.

For simulations with point seeds, there are no FSCs at all, provided the lattice is large enough so that its boundary is never hit. The latter was checked in each run.

For infinite seeds we used periodic boundary conditions (length L) in the direction of the seed extension(s). Let us call a point y an 'ancestor' of a space–time point (x, t) if there is a spreading path from y to x of length $\leqslant t$. It is easy to see that FSCs are proportional to the probability that any point (x, t) has two ancestors y_1 and y_2 which are a distance L apart. Indeed, a configuration on a finite lattice with periodic boundary conditions can be viewed as a special—periodic—configuration on an infinite lattice. This periodicity (which is the only possible source of FSCs) can only be felt if a point has two ancestors which are in identical states due to the periodicity. For line seeds, we could use lattices longer than the maximal diameter of any cluster measured with point seeds (with comparable statistics), ruling thus out any sizeable FSCs. In general the aspect ratio (length/width) of the lattice was about 2.

For plane seeds, the above criterion would have required somewhat too large lattices. But notice that the above estimate is somewhat pessimistic and can be refined. A more careful argument shows that FSCs can arise only if the following holds for some $t > 0$: together with *each* ancestor y of (x, t), also one of the four points $y \pm Le_i$ is an ancestor of (x, t). Here e_1 and e_2 are unit vectors in the seed plane. If this does not hold (i.e. if for each (x, t) one of the ancestors is unpaired), then this unpaired ancestor would have already wetted (x, t), and this would be independent of any periodicity. We estimated that with our lattice sizes and growth times ($L = 512$, $t \leqslant 1500$) the resulting FSCs are negligible.

(*b*) In addition to these simulations where the spreading was followed in real time as in an epidemic process, I used also a depth-first algorithm as given in [19]. This is somewhat faster than the breadth-first algorithm described above, but it does not give observables as functions of spreading time. It was thus used only in an application where following the real-time evolution would not have made sense in any case. These runs were devoted to measuring directly the surface exponent β_s/ν appearing in equation (28). For this, I used a lattice of size $L \times L \times h$ with $L \gg h$. What was measured was the number of sites on the upper surface $z = h$ wetted by the entire lower surface $z = 0$ taken as seed. Lateral boundary conditions were again taken periodic. For this purpose, h was first put to 1, spreading was run until all wettable sites had been wetted, and all wetted sites on the upper boundary were written in a list. After that, the height was increased to $h = 2$, the previous list of wetted boundary sites was taken as the new seed, and spreading was continued until again all sites were wetted. This was repeated, each time increasing h by one unit and using

the old list of wetted sites as new seeds, until the maximal hight was reached. In this way the surface 'order parameter' was measured in a single run for all heights up to $h = 255$, on surfaces of size 640. The statistics accumulated this way was several orders of magnitude larger than that of [16].

For these last simulations, the above arguments against FSCs are not helpful since we do not have any control of the spreading times, and they can occasionally be very large. To estimate FSCs in this case, we thus also ran simulations on smaller lattices. Results from such a check will be given later together with the main results.

(*c*) All simulations reported below were done in the close vicinity of the percolation thresholds: for bond percolation, we used $0.2878 \leqslant p \leqslant 0.2884$, while for site percolation $0.31155 \leqslant p \leqslant 0.3117$. These intervals are large enough that they span the uncertainty of p_c, and thus allow estimates of it. On the other hand, they are so small that the dependence of the observables on p is still linear, and hence averages can be formed by averaging over p.

The entire statistics is found in table 1, together with the average CPU times per run. The total CPU time spent on these simulations was somewhat more than 4700 h.

Table 1. 'Type' indicates bond (b) and site (s) percolation, respectively. 'Lateral size' indicates the size of the lattice in the direction of the seed, unless the latter is a point. The last two lines (wetted surface sites) refer to simulations using the depth-first algorithm discussed at the end of section 3. For them, the first column refers to the thickness h of the layer, while for all other simulations the first column gives the number t of time steps.

No	Seed (observable)	Type (b/s)	t resp. h	Lateral size	CPU time (s/run)	Number of runs
1	Point	b	800	—	0.37	4 800 000
2		s	750	—	0.73	2 900 000
3	Line	b	700	768	19	60 000
4		s	650	768	25	84 000
5	Plane	b	1500	512 x 512	75	8 500
6		s	1400	512 x 512	96	7 100
7	Surface point	b	1100	—	0.09	26 000 000
8		s	1100	—	0.13	15 000 000
9	Surface line	b	1050	1024	9.1	43 000
10		s	1000	1024	9.8	44 000
11	Edge point	b	1500	—	0.0076	44 000 000
12		s	1500	—	0.0156	18 000 000
13	Edge line	b	1500	768	1.8	340 000
14		s	1500	896	1.93	250 000
15	Surface, Wetted surface sites	b	255	640 x 640	140	10 700
16	"	s	255	640 x 640	160	4 800

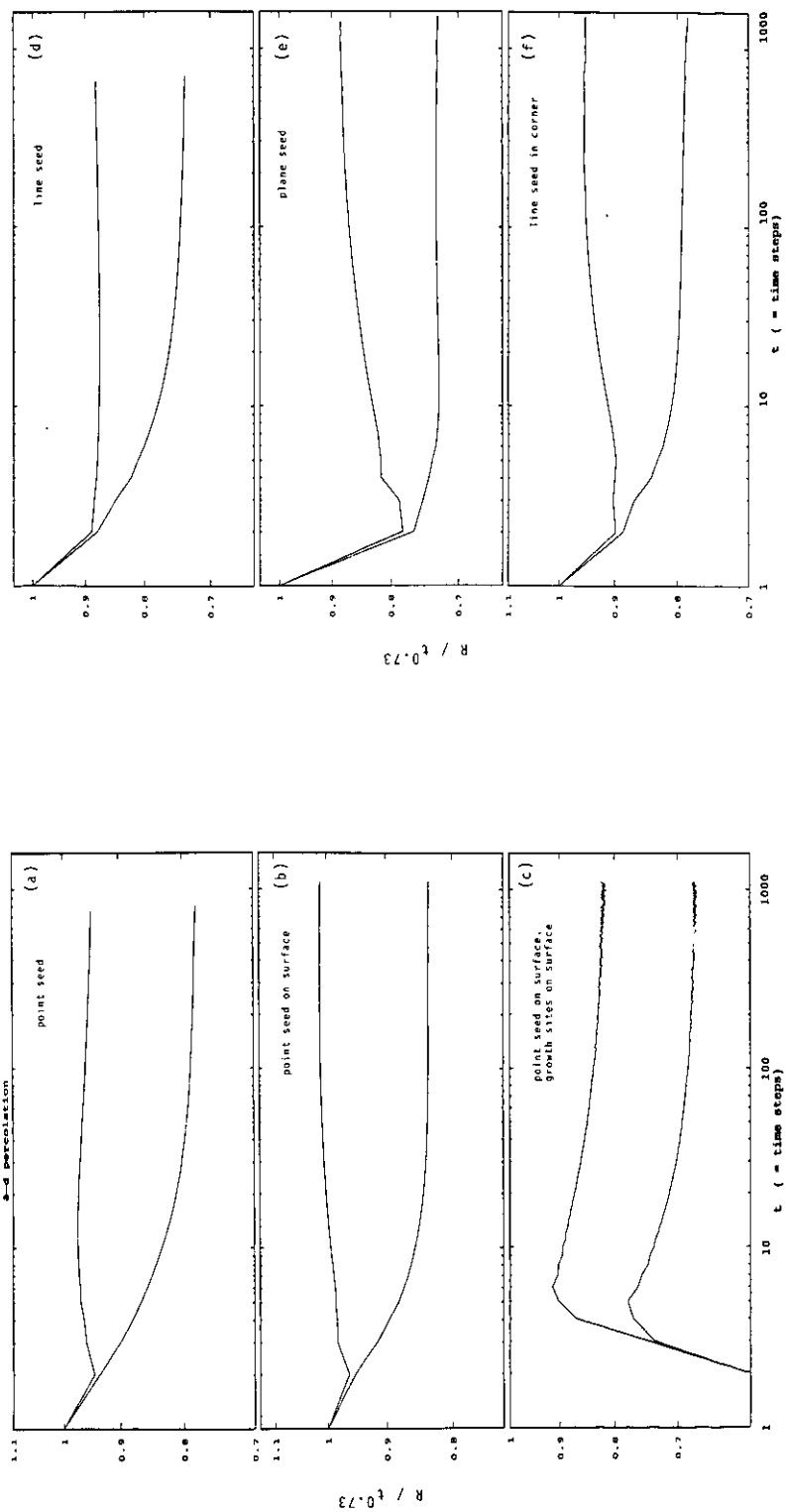

Figure 3. Distances of growth sites from the seed, for the six geometries with most relevant results. In each panel, the upper curve is for site percolation, and the lower for bond. In order to enhance the significance, we show $R(t)/t^{0.73}$ against t on doubly logarithmic scales. In panel (*e*) the average distance from the seed plane is shown, in all other panels the RMS distances $\langle R^2\rangle^{1/2}$. The statistical error bars are smaller than the thickness of the lines, except for panels (*c*) and (*f*). For panel (*c*) they are as indicated by the visible jitter, while for the last two panels they reach 0.1% for the largest values of t.

4. Results

4(a) *Exponent* z. In figure 3 we show the distances $R(t)$ for the six most relevant sets of growth sites. On each panel both bond and site results are shown. In order for the graphs to be more significant, we have divided off the dominant power behaviour $t^{0.73}$, and show the ratios $R/t^{0.73}$ on log–log plots. In all panels the upper curves refer to site percolation, while the lower ones refer to bond percolation. As we had already pointed out in the introduction, $R(t)$ depends very little on the precise value of p. The curves shown in figure 3 represent averages over all p, with the average p very close to 0.248 8125 resp. 0.311 605. If we had superimposed the individual results for each p, the curves would have thickened only very little.

Panel (b) shows the distance of growth sites on a *surface* (from a point seed on the same surface). The fact that we see the same power behaviour as in the other panels (where growth sites in the bulk are used) is our best proof for the claim that z is the same on surfaces and in the bulk.

Except in panels (b), (e) and (f), the statistical errors are less than the widths of the lines. In panel (b), the uncertainties are just as large as the visible jitter, while the errors in panels (e) and (f) are up to 0.1%. With these caveats, all trends visible in figure 3 are thus statistically significant. In particular, we see in panel (d) that the site percolation results from line seeds clearly indicate that $z > 0.73$ (as was also clear from figure 2): not only has the upper curve a positive slope for large t, it is also curved upward. Similar upward curvatures are seen in panels (a) and (c). In panel (b) the bond result looks very straight and the site result is slightly curved downward. Clear downward curvatures are seen in panels (e) and (f). In addition, the bond

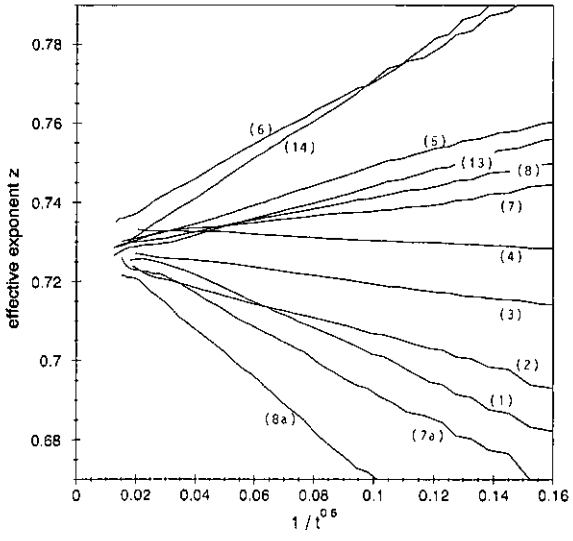

Figure 4. Effective exponents for the increase of the growth site distances. As in figure 2, fits to the derivatives $\mathrm{d}\log R/\mathrm{d}\log(t - t_0)$, fitted over two octaves, are plotted against $1/t^{0.6}$. The values of t_0 are chosen such as to produce the straightest lines. Each line corresponds to one geometry (with the numbers corresponding to those in tables 1 and 2), and to an average over all values of p in the vicinity of p_c. In these averages care was taken to obtain averages of p equal to the values of p_c given in [6]. Statistical errors can be estimated by comparing with figure 2 and with the errors of the extrapolations to $t \to \infty$ given in table 1.

percolation results in the latter panels show already significant negative slopes, which together with the downward curvature would clearly indicate $z < 0.73$.

Local effective exponents obtained from the data shown in figure 3 are given in figure 4. From equation (2) we would have

$$\frac{\mathrm{d}\log R(t)}{\mathrm{d}\log t'} = z + (z - \Delta - 1)b/t'^{\Delta} + \ldots \tag{30}$$

with $t' = t - t_0$. Thus we plotted $\mathrm{d}\log R(t)/\mathrm{d}\log t'$, obtained by fitting over intervals $[t/4, t]$, against $1/t'^{\Delta}$. If equation (2) is correct and t_0 was chosen optimally, we would get straight lines. We indeed see reasonably straight lines in figure 4, with a value $\Delta = 0.6$ compatible with previous analyses [11, 12]. We should however point out that the origin from which R is to be measured is not always uniquely defined. Allowing an uncertainty δR of order 1 in the definition, the scaling ansatz should read $R \approx \delta R + At^z \approx At^z(1 + \text{constant}t^{-z})$, mimicking thus a non-analytic correction with exponent $\Delta \approx 0.73$. It is possible that the observed Δ is strongly influenced by this.

But the intercepts of these lines at $1/t = 0$ do not coincide. These should be the true critical exponents. Their values are given in the first column of table 2. Notice that the fits were made for each data set separately, i.e. no consistency between the lines of table 2 were imposed. The errors there are somewhat subjective, as is usual in such extrapolations. This could of course mean that universality and/or hyperscaling is violated, but we prefer to interpret it as evidence for further corrections to scaling which would be explicitly visible only with much higher statistics.

Thus no simple ansatz for the corrections to scaling is possible which could describe all data shown in figures 3 and 4 consistently. On the other hand, the discrepancies are very small. Each curve is compatible with z being not more than two standard deviations away from the value

$$z = 0.728 \pm 0.003 \tag{31}$$

which we take as our preliminary estimate.

Previous estimates of this exponent were, among others, 0.725 ± 0.006 [11], 0.728 ± 0.006 [12], 0.70 ± 0.01 [20] and 0.746 ± 0.0056 [21]. The latter had consumed by far the largest amount of CPU time (about 5000 h CPU time on an IBM 3091 mainframe), but seems to be off by more than 2 standard deviations.

4(*b*) *Exponents y, δ; bulk behaviour.* In contrast to $R(t)$, both $N_g(t)$ (resp. $n_g(t)$) and $P(t)$ are strongly dependent on p. This suggests two possible strategies. In view of the fact that our total statistics is smaller than that of [6], we can accept their estimates of p_c, and obtain estimates of y and δ with very small statistical error bars. Alternatively, we can try to fit the exponents together with p_c. In table 2 we show results of the first kind of fit, in table 3 the latter. For both tables notice that y depends on the seed, in contrast to z, and that δ is non-zero only for point seeds.

Compared with $R(t)$, both $n_g(t)$ and $P(t)$ have in general more complicated *visible* corrections to scaling, i.e. no straight lines are in general obtained when plotting the logarithmic slopes against any negative power of t with an exponent close to 0.6. As examples we show in figure 5 the effective exponents for the numbers of growth sites from point seeds on surfaces (panel (*a*)), and from line seeds (panel (*b*)).

Table 2. Critical exponents obtained by assuming p_c given by the values of [6], $p_c = 0.248\,8125 \pm 0.000\,0010$ (bond) resp. $0.311\,605 \pm 0.000\,010$ (site). Numbers in brackets give statistical errors in the last digits.

No	Seed (observable)	Type	z	y	δ resp. δ_s, δ_e	β_s/ν	Scaling relation
1	Point	b	0.730(3)	0.488(4)	$\delta = 0.345(4)$	—	$y_{point} + 2\delta - 3z + 1 = -0.012(12)$
2		s	0.729(3)	0.500(6)	δ=0.342(5)	—	$= -0.003(13)$
3	Line	b	0.7284(11)	0.107(5)	—	—	$y_{line} + \delta - 2z + 1 = 0.005(8)$
4		s	0.734(1)	0.115(18)	—	—	$= 0.001(20)$
5	Plane	b	0.7275(15)	−0.619(4)	—	—	$y_{plane} + \delta - z + 1 = -0.002(7)$
6		s	0.729(2)	−0.618(7)	—	—	$= -0.003(8)$
7	Surface point	b	0.7290(15)	0.127(4)	$\delta_s = 0.710(4)$	—	$y_{surf} + \delta + \delta_s - 3z + 1 = -0.005(8)$
8		s	0.728(1)	0.143(13)	$\delta_s = 0.693(4)$	—	$= -0.003(14)$
7a	Surface point, (surface growth sites)	b	0.733(3)	−0.96(1)	—	—	$y_{surf,surf} + 2\delta_s - 2z + 1 = -0.006(13)$
8a		s	0.731(4)	−0.945(15)	—	—	$= -0.020(17)$
9	Surface line	b	0.7245(15)	0.11(7)	—	—	$y_{surf\ line} - \min\{y_{line}, y_{surf}\} = -0.00(7)$
10		s	0.723(3)	0.07(6)	—	—	$= -0.04(7)$
11	Edge point	b	0.727(3)	−0.301(4)	$\delta_e = 1.133(6)$	—	$y_{edge} + \delta + \delta_s - 3z + 1 = -0.004(11)$
12		s	0.724(5)	−0.30(1)	$\delta_e = 1.13(1)$	—	$= 0.002(20)$
13	Edge line	b	0.725(2)	−0.304(6)	—	—	$y_{edge\ line} + \delta + \delta_s - 3z + 1 = -0.001(12)$
14		s	0.723(2)	−0.300(12)	—	—	$= 0.005(18)$
15	Plane (density of wetted surface sites)	b	—	—	—	0.972(7)	$\beta_s/\nu - \delta_s/z = -0.001(10)$
16		s	—	—	—	0.985(10)	$= 0.035(15)$

Table 3. Critical exponents y, δ and β_s/ν obtained by letting p_c float, together with the values obtained thereby for p_c. Due to its weak dependence on p_c, the exponent z is the same as in table 2 and is not shown again. In order to reduce the uncertainties, we demanded in the fits that bond and site percolation give the same exponents for the same geometry and observable. Consistency among different geometries was however not demanded.

No	Seed (observable)	Type	p_c	y	δ resp. δ_s, δ_e	β_s/ν	Scaling relation
1	Point	b	0.248 819(6)			—	$y_{\text{point}} + 2\delta - 3z + 1 = -0.001(12)$
2		s	0.311 595(10)	0.493(3)	$\delta = 0.345(4)$	—	
3	Line	b	0.248 816(5)				$y_{\text{line}} + \delta - 2z + 1 = 0.001(8)$
4		s	0.311 60(2)	0.110(5)	—	—	
5	Plane	b	0.248 811(4)				$y_{\text{plane}} + \delta - z + 1 = -0.000(8)$
6		s	0.311 615(15)	−0.617(5)	—	—	
7	Surface point	b	0.248 822(4)			—	$y_{\text{surf}} + \delta + \delta_s - 3z + 1 = -0.009(11)$
8		s	0.311 590(6)	0.130(4)	$\delta_s = 0.700(4)$	—	
7a	Surface point (surface growth sites)	b	—		—	—	$y_{\text{surf,surf}} + 2\delta_s - 2z + 1 = -0.006(13)$
8a		s	—	−0.950(8)	—	—	
9	Surface line	b	0.248 82(6)		—	—	$y_{\text{surf line}} - \min\{y_{\text{line}}, y_{\text{surf}}\} = -0.02(5)$
10		s	0.311 61(2)	0.09(5)	—	—	
11	Edge point	b	0.248 812(5)				$y_{\text{edge}} + \delta + \delta_e - 3z + 1 = -0.006(11)$
12		s	0.311 61(2)	−0.300(4)	δ_e=1.133(6)	—	
13	Edge line	b	0.248 808(4)				$y_{\text{edge line}} + \delta + \delta_e - 3z + 1 = -0.008(13)$
14		s	0.311 60(2)	−0.302(10)	—	—	
15	Plane (density of wetted surface sites)	b	0.248 812(4)	—	—		$\beta_s/\nu - \delta_s/z = 0.013(12)$
16		s	0.311 60(2)	—	—	0.975(10)	

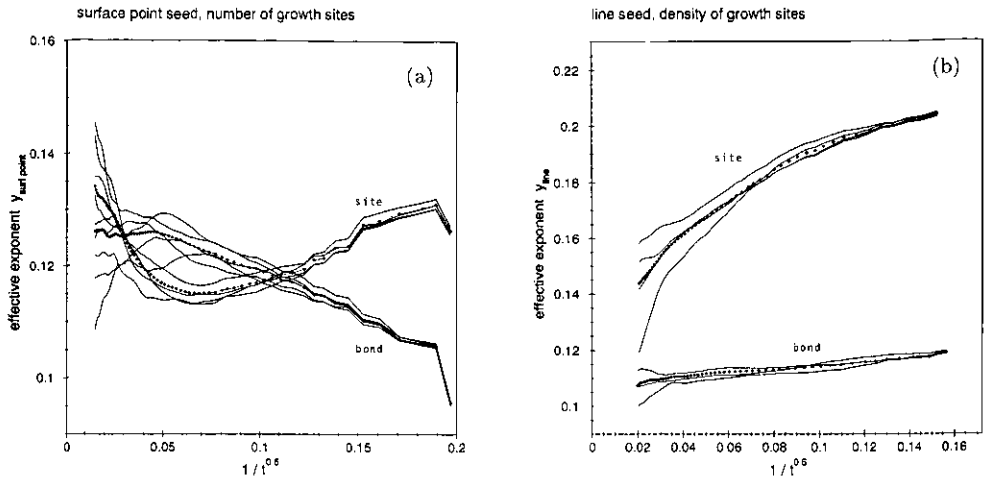

Figure 5. Effective exponents for the number (resp. density) of growth sites. The data were obtained by fitting straight lines to $\log N_g/\mathrm{d}\log t$ as in figure 2. No constant offset t_0 was subtracted from t, since no straight lines would have been obtained for any t_0. In panel (a) the seed was a point on a surface, while in panel (b) it was a line. The values of p are in panel (a) $p = 0.31159, \ldots, 0.31163$, resp. $p = 0.24888, \ldots, 0.24883$, both in steps of 0.00001. In panel (b) the curves are for $p = 0.31155$, 0.31160, 0.31162 and 0.31165, resp. $p = 0.24888$, 0.24881 and 0.24882. The dots correspond again to averages.

We have to add one comment on the estimate of $y_{\mathrm{surf\ line}}$ in lines 11 and 12 of tables 2 and 3. Though this is strictly speaking not a bulk exponent, the relation $y_{\mathrm{surf\ line}} = \min\{y_{\mathrm{surf}}, y_{\mathrm{line}}\}$ puts a strong constraint on it in terms of bulk exponents and vice versa. By plotting the logarithmic derivative $\mathrm{d}\ln n_g/\mathrm{d}\ln t$ for growth from a surface against $1/t^{\Delta}$, we find straightest lines for $\Delta \approx 0.15$–0.2 (see figure 6). Such small Δ implies however that the true exponent is obtained by a very long extrapolation, and has thus very large uncertainties. Also, the offset t_0 needed to produce a straight line for the site percolation data was $t_0 \approx 8$, indicating that a fit with a single non-analytic correction term is not very meaningful. Similarly large corrections to scaling are also responsible for the very large errors quoted for some of the other exponents in table 2.

Comparing tables 2 and 3 we see few differences. In general the estimates for p_c in table 3 are very close to those of [6]. Our best overall estimates (using in addition the simulations to be discussed in the next subsection) are

$$p_c = 0.248\,814 \pm 0.000\,003 \qquad \text{(bond percolation)} \tag{32}$$

and

$$p_c = 0.311\,604 \pm 0.000\,006 \qquad \text{(site percolation)}. \tag{33}$$

Imposing the correct scaling relations, our overall estimates for the bulk exponents are finally

$$z = 0.728 \pm 0.002 \qquad y = 0.494 \pm 0.006 \qquad \delta = 0.345 \pm 0.004. \tag{34}$$

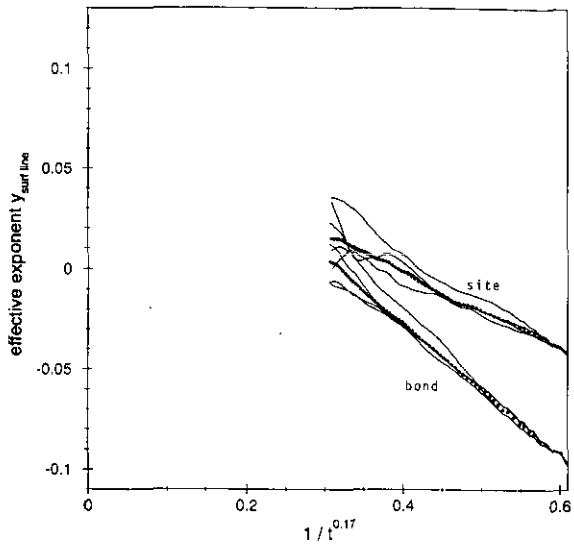

Figure 6. Similar to figure 5, but for a line seed on a surface, and plotted against $1/t^{0.17}$. Also, constants t_0 were used as in figure 2 to produce straight lines. The curves correspond to $p = 0.31158$, 0.3116, 0.31162 and 0.31165, resp. $p = 0.24888, \ldots, 0.24883$.

Exponents derived from these are $\eta = 2\beta/\nu - d + 2 = 2\delta/z - 1 = -0.052 \pm 0.009$ and $D_t = d - \beta/\nu = 3 - \delta/z = 2.526 \pm 0.006$. They are in very good agreement with the more precise estimates of [6].

In conclusion we can say that the determination of y and δ is less precise than that of z. But it is less problematic, not because the scaling corrections are smaller, but because they are already visible at the present lattice sizes. For z there must be scaling corrections which should show up only much later, and whose existence is only indicated indirectly internal inconsistencies.

Finally, I want to make a short comment on the supercritical behaviour. For $p > p_c$, we expect n_g to tend towards a positive constant with $t \to \infty$, when starting with a plane seed. Naively one might have expected this convergence to be monotonic, since n_g decreases also monotonically at $p = p_c$. But as seen in figure 7 (and observed already in [11] for $d = 4$), this is not true. For a plane seed, n_g first goes through a minimum before settling towards a constant (we cannot exclude even further oscillations). *A posteriori*, this can be explained easily. The decrease of n_g for a plane seed is a result of two competing effects: on the one hand, the growth surface becomes more and more wrinkled with time, and thus its area increases. On the other hand, the density of growth sites on this wrinkled surface decreases, and actual growth is restricted to fewer and fewer subdomains. Figure 7 shows that the latter effect dominates at small times (and for $p = p_c$ at all times), but that the wrinkling effect dominates at large times for $p > p_c$.

4(*c*) *Surface and edge exponents.* The simulations with seeds on surfaces and on edges, and with the spreading followed in 'real' time, were analysed exactly as those with seeds in the The results are also given in tables 2 and 3. As seen from these tables, the internal consistency of these results is quite good. They give the estimates

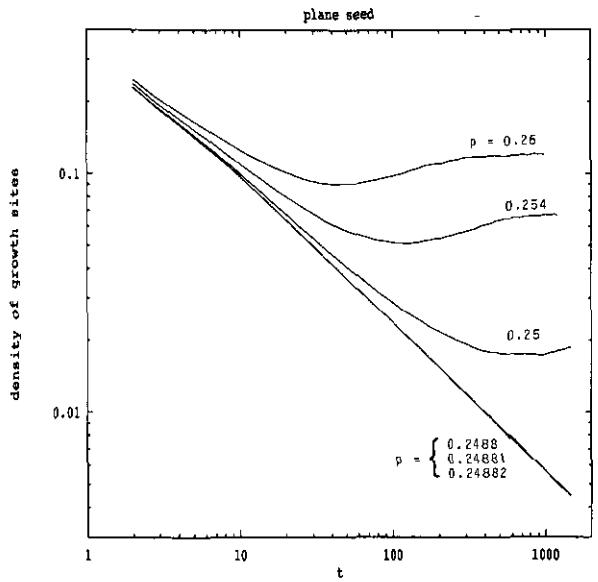

Figure 7. Density of growth sites for bond percolation using a seed which consisted of an entire plane, plotted against t. What looks like a straight line is actually three curves for $p = 0.2488$, 0.248 81 and 0.248 82. For $p_c \geqslant 0.25$ one sees that n_s goes through a minimum, before tending towards a constant for $t \to \infty$.

$$\beta_s/\nu = \delta_s/z = 0.966 \pm 0.007 \qquad \beta_e/\nu = \delta_e/z = 1.56 \pm 0.01. \quad (35)$$

The depth-first simulations (reported in the last lines of tables 2 and 3) were the only simulations where we could not exclude finite-size corrections *a priori*. Thus we have also performed simulations on a lattice with much smaller base surface than that of our main simulations ($L \times L = 160 \times 160$ instead of 640×640). In figure 8 we show the number of wetted sites against the thickness h of the layer, both for the main simulations and for these test runs. We see that the finite-size corrections are negligible for $h < 0.4L$, suggesting thus that we can believe our simulations up to $h = 256$. The resulting exponents are also given in tables 2 and 3, and our final estimate for β_s is

$$\beta_s/\nu = 0.970 \pm 0.006. \quad (36)$$

This should be compared with the best previous estimate, $\beta_s/\nu = 0.98 \pm 0.02$ of [16]. The fractal dimension of wetted surface sites becomes from this $D_{f,s} = d - 1 - \beta_s/\nu = 1.030 \pm 0.004$. This is indeed slightly larger than 1, in agreement with our finding that $y_{\text{surf line}} = y_{\text{line}}$.

5. Conclusions

In this paper we have presented Monte Carlo results for the spreading of percolation in three dimensions. In order to check for systematic corrections to scaling, we have compared bond and site percolation, and we have measured in many different

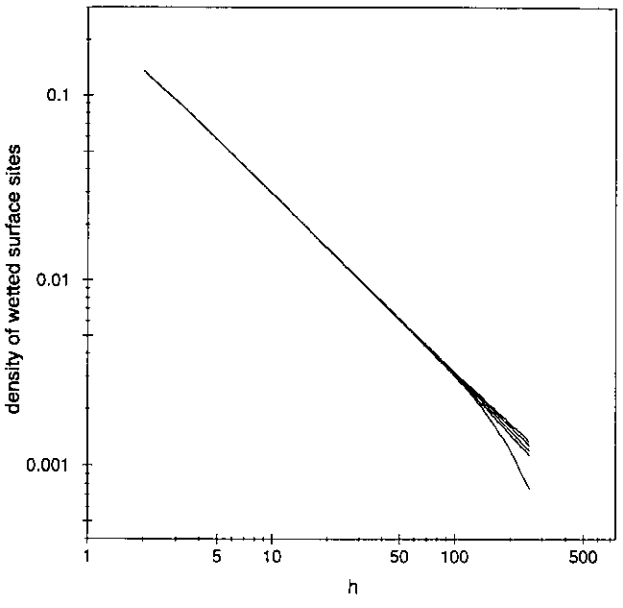

Figure 8. Density of wetted surface sites for bond percolation starting from the opposite surface of a slab-shaped lattice, plotted against the thickness h of the slab. In contrast to all previously shown figures, these data were obtained by means of the depth-first algorithm described at the end of section 3. The upper four curves are for $p = 0.24878, \ldots 0.24884$ in steps of 0.00002, on lattices with surface 640 x 640. The lowest curve is for $p = 0.2488$ on a surface of only 160 x 160 sites.

geometries. Except for the last set of data, we have also measured in each case more than one observable.

In particular we have also measured the spreading in the vicinity of surfaces and edges. This gave us, in addition to the bulk exponents, also estimates of the surface resp. edge exponents. In order to compare the exponents of different observables in different geometries, we have formulated new heuristic (hyper-)scaling laws which were tested with high precision.

Compared with previous simulations, our statistics is outpassed only by those of [6] (who did not measure spreading and surface exponents) and those of [2], who measured indeed none of the present observables. Compared with all other studies, the present one gives *statistical* errors which are smaller by at least one order of magnitude. Our quoted final errors show much less improvement due to the very substantial systematic corrections to scaling which went unnoticed in previous work.

We verified previous claims [11] that the distance $R(t)$ involved a correction-to-scaling exponent $\Delta \approx 0.6$ with large amplitude. But we found that this cannot be the leading correction. Otherwise our data would not be internally consistent: in addition to breaking of universality in the usual sense, we would have no universality between exponents measured in different geometries.

For the second independent critical bulk exponent we found similarly large corrections to scaling. In that case, one could indeed see from some of the individual measurements that a very small correction-to-scaling exponent is needed. A precise measurement was impossible since this seemed not to be the only such exponent less

than 1. The latter is in contrast to claims in [10] (for different observables), where only analytic corrections to scaling were found in addition to logarithmic ones. were found in addition to logarithmic ones.

The same remarks apply to the surface exponent β_s. Finally, we also measured the analogous edge exponent β_e. We found that the fractal dimension of wetted surface sites is slightly larger than 1, and that the fractal dimension of wetted edge sites is definitely less than 0. This agrees with previous findings [12], and means that the probability for an edge of a cube to intersect the largest cluster tends to zero when its size tends to ∞.

An important result of our simulations is that there is only a single independent surface exponent, and (for any fixed angle) a single edge exponent. *A priori* one might have thought that a second independent surface exponent is needed for spreading, but our simulations showed clearly that this is not the case.

In [11] only planes were used as seeds. It was argued that point seeds in particular should be less efficient since they induce large fluctuations at early stages of the growth (where the number of growth sites per cluster is very small), and that these fluctuations influence the measurements also at later times. This is true, but it is only part of the full truth. Another effect is that with large seeds (planes, lines) one spends much more time on small clusters which contribute little to understanding the scaling region. If one uses point seeds, the probability for a randomly chosen seed to be on a cluster of size N is proportional to N, thus suppressing small clusters. We found that both effects essentially cancel. The statistical errors on the exponents obtainable with fixed CPU time are very much independent of the type of seed.

Our results show that one has to be very careful when using spreading for estimations of critical percolation exponents, though it seems to be by far the most efficient algorithm as far as speed is concerned. In order to go substantially beyond the present investigations, one would have to use not only larger clusters but also much higher statistics. Only then one could hope to fix precisely the scaling corrections, and to obtain reliable extrapolations to the critical point.

Acknowledgments

This work was supported by the Deutsche Forschungsgemeinschaft, SFB 237. It is a pleasure to thank Robert Ziff for very useful correspondence and S Dietrich for discussions.

References

[1] Stauffer D 1985 *Introduction to Percolation Theory* (London: Taylor and Francis)
[2] Normand J M and Herrmann H J 1990 *Int. J. Mod. Phys.* C **1** 207
[3] Gingold D B and Lobb C J 1990 *Phys. Rev.* B **42** 8220
[4] Roman H E 1990 *J. Stat. Phys.* **58** 375
[5] Duering E and Roman H E 1991 *J. Stat. Phys.* **64** 851
[6] Ziff R M and Stell G 1988 *Critical behavior in three-dimensional percolation: is the percolation threshold a Lifshitz point?, Michigan preprint*; and private communication
[7] Broadbent S R and Hammersley J M 1957 *Proc. Camb. Phil. Soc.* **53** 629
[8] Mollison D 1977 *J. R. Stat. Soc.* B **39** 283
[9] Grassberger P 1983 *Math. Biosci.* **62** 157
[10] Sahimi M and Arbabi S 1990 *J. Stat. Phys.* **62** 453

[11] Grassberger P 1986 *J. Phys. A: Math. Gen.* **19** 1681
[12] Grassberger P 1986 *J. Phys. A: Math. Gen.* **19** L241
[13] Diehl H W 1986 *Phase Transitions and Critical Phenomena* vol 10, ed C Domb and J L Lebowitz (New York: Academic)
[14] Janssen H K, Schaub B and Schmittmann B 1988 *J. Phys. A: Math. Gen.* **21** LA27
[15] Diehl H W and Lam P M 1989 *Z. Phys.* B **74** 395
[16] Hansen A, Lam P M and Roux S 1989 *J. Phys. A: Math. Gen.* **22** 2635
[17] Leath P L 1976 *Phys. Rev.* B **14** 5046
[18] Kirkpatrick S and Stoll E P 1981 *J. Comput. Phys.* **40** 517
[19] Wang J-S and Swendsen R H 1990 *Physica* A **167** 565
[20] Neumann A U and Havlin S 1988 *J. Stat. Phys.* **52** 203
[21] Herrmann H J and Stanley H E 1988 *J. Phys. A: Math. Gen.* **21** L829